

Deformation and Failure of Rock Samples Probed by NMR Relaxometry

C.H. van der Zwaag¹, E. Veliyulin¹, T. Skjetne¹, A.E. Lothe², R.M. Holt², O.M. Nes²

¹SINTEF Unimed MR-Center, N-7465 Trondheim, ²SINTEF Petroleum Research, N-7465 Trondheim

Abstract

The objective of the study was to pinpoint the effect of stress induced rock matrix alterations on NMR-wireline-log measurements by means of laboratory T1 and T2 relaxation time measurements; here comprehensively termed NMR-Relaxometry (NMRR). The research activities were subdivided into two major parts: (1) NMR measurements on an outcrop sandstone during uniaxial compressional tests and (2) NMR measurements on artificial sandstone samples prepared with defined crack patterns.

T1-measurements performed on core plug samples (Red Wildmoor Sandstone) during compaction showed a clear and consistent decrease in the relaxation rate up to a point assumed to characterise the yield strength. The rate decreased most probably as a result of the compaction of micropores. As micropores disappeared mean T1-relaxation times shifted to greater values, i.e the relaxation rates decreased. This trend was reversed when the rock failed. The relaxation rate increased again, most probably through the generation of fresh mineral surfaces at broken cementations or grain contacts.

Controlled crack volumes and the T2-relaxation rate correlated well for artificial sandstone samples. It is shown that relaxation rates were affected by a change in the contribution of self-diffusion to the total proton relaxation. Increasing crack volumes showed significant increases in the self diffusion coefficient, D , of the pore fluid. Relaxation rates increased because of increases in D . This observation is in contrast to the initial assumption that cracks would induce slower relaxation (greater mean relaxation times) as they create open spaces in the porous matrix that would correlate to larger pores.

The study may serve as a first tool to assess the potential error in the interpretation of NMR downhole measurements performed in formations affected by stress induced cracks or fissures. It may also be helpful to demonstrate and explain dependencies between rock mechanical parameters, routine core analysis measurements and NMR-measurements.

Introduction

NMR well-logging measurements probe the wellbore environment at a short distance from the wellbore wall in order to isolate productive zones and to assess reservoir volume and flow capacity. However, the rock properties in this near wellbore zone may be altered by the mechanical impact of the drilling process or physicochemical interaction between the drilling fluid and the rock formation.

While the latter has been a major issue in recent research (van der Zwaag *et al.*, 2000), little attention has been given to the effect of stress-induced cracks or fissures on NMR signal response. However, stress re-distribution around a wellbore due to the excavation of rock masses initiates the deformation of the rock matrix and causes subsequent failure, particularly in the near-wellbore environment. The generation of micro fissures or cracks due to failure effects in next instance petrophysical parameters such as the rock porosity, pore size

distributions and rock permeability. Downhole NMR-measurements performed in zones where such petrophysical properties are altered by stress induced effects may therefore not be representative and provide misleading information in formation evaluations.

On the other hand, while negative effects may lead to faulty log interpretation, logging signals may in contrast contain information about the stress state around the wellbore as well as how anisotropies may affect the productivity of the wellbore.

Objective and Scope

The objective of the study was to gain an initial perception of stress induced rock matrix alterations and their effect on NMR-wireline-log measurements. To approach the objective two separate studies were performed:

1. NMR relaxation time measurements on sandstone samples under stress.
2. NMR relaxation time measurements on artificial sandstone samples prepared with defined crack pattern.

NMR Relaxation Time Measurements

NMR relaxation time measurements on fluid filled porous systems (rocks) provide information on how the rock matrix interacts with fluids and the properties of the fluids themselves. NMR measurements are evaluated based on equations describing the relaxation rate of the hydrogen protons in terms of their longitudinal (T_1) and transversal (T_2) relaxation time (e.g. Kleinberg *et al.*, 1993).

T_1 is typically measured as the build-up of the longitudinal magnetisation in an inversion recovery measurement. The relaxation rate $1/T_1$ is the sum of the relaxation rate of the bulk fluid $1/T_{1B}$ as well as the product of surface relaxivity r_1 and surface to volume ratio S/V :

$$\frac{1}{T_1} = \frac{1}{T_{1B}} + r_1 \left(\frac{S}{V} \right) \dots \dots \dots (1)$$

The transversal relaxation rate $1/T_2$ is, similar as $1/T_1$, the sum of: relaxation rate of the bulk fluid $1/T_{2B}$ and the product of surface relaxivity ρ_2 and surface to volume ratio S/V . In addition T_2 is affected by self-diffusion of the protons. This adds a diffusion depending component to the rate equations:

$$\frac{1}{T_2} = \frac{1}{T_{2B}} + r_2 \left(\frac{S}{V} \right) + \frac{D\gamma^2 G^2 TE^2}{12} \dots \dots \dots (2)$$

where D is the Self diffusion coefficient, γ is the gyromagnetic ratio of the ^1H proton, G is the Internal field gradient, and TE the Interecho spacing.

To reduce data, eq. 1 was transformed. As the measurements presented below were performed on the same rock sample and as the pore fluid was not changed during the measurements, it was assumed that the contribution of the relaxation rate of the bulk fluid, $1/T_{1B}$, remained unchanged by the axial stress imposed on the rock sample in a drained state. "Drained conditions" means that there is no pore pressure allowed to build up and that, hence, the density of the pore fluid remains unaltered. Constant density and unaltered composition are requirements for constant $1/T_{1B}$, which ultimately allows us to reduce data produced by two successive T_1 measurements under different axial loads but otherwise constant conditions according to:

$$\Delta \frac{1}{T_1} = \frac{1}{T_{1,n}} - \frac{1}{T_{1,0}} = r_{1,n} \left(\frac{S_n}{V_n} \right) - r_{1,0} \left(\frac{S_0}{V_0} \right) \dots \dots \dots (3)$$

The index 0 denotes a reference point measurement and the index *n* a subsequent measurement.

For the second part of the study, “Measurements on artificial sandstone samples”, a similar approach was used. Observing differential relaxation rates on a system investigated by T2 measurements at two different interecho spacings, *TE*, allows to derive eq. 4. The relaxation rate of the bulk fluid, $1/T_{2B}$, and the surface relaxivity, r_2 , as well as the surface to volume ratio, *S/V*, are constant at different interecho spacings. Subtracting two measurements from each other yields the relaxation rate difference:

$$\Delta \frac{1}{T_2} = \frac{1}{T_{2,n}} - \frac{1}{T_{2,0}} = \frac{Dg^2}{12} (G_n^2 TE_n^2 - G_0^2 TE_0^2) \dots\dots\dots(4)$$

Resolving eq. 4 to the diffusion coefficient, *D*, yields eq. 5:

$$D = 12 \frac{\left(\frac{1}{T_{2,n}} - \frac{1}{T_{2,0}} \right)}{g^2 (G_n^2 TE_n^2 - G_0^2 TE_0^2)} \dots\dots\dots(5)$$

CPMG measurements with varying interecho spacings have been presented by Coates *et al.* (1993) as a means to measure the diffusion coefficient of the pore fluids confined in petroleum reservoir rock through downhole NMR wireline logging measurements.

Measurements on Sandstone Samples Under Stress

Method

To observe the effect of compression and failure on NMR relaxation time, a NMR-spectrometer was integrated into rock mechanical test equipment. The drawing in Fig. 1 illustrates the measurement set-up. Rock mechanical measurements were performed as drained, uniaxial compression tests.

¹H-NMR- measurements at 2 MHz proton resonance frequency were performed on water saturated Red Wildmoor sandstone samples at otherwise ambient conditions. Water was degassed before use. Measurements on rock samples were performed under increasing axial load.

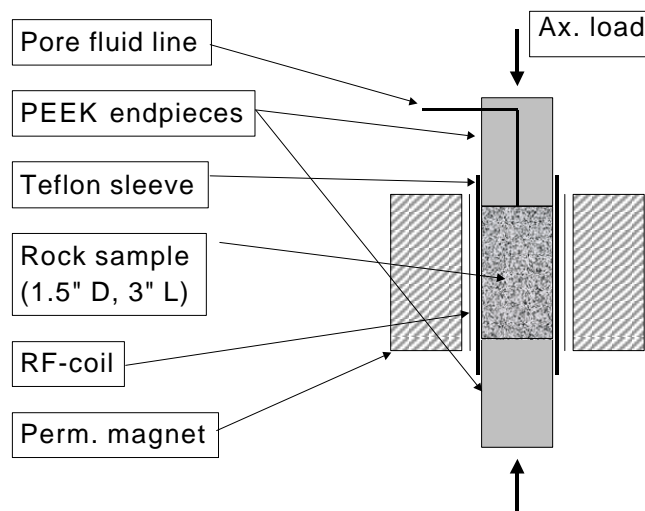


Fig. 1. Principle set-up of NMR-measurements during rock-mechanical measurements.

The longitudinal relaxation time T_1 (spin-lattice-relaxation) was measured using the inversion recovery pulse sequence. 30 delay times equally spaced on a logarithmic scale from 0.1 to 10 s were used to record the time dependence of the NMR signal recovery. The transverse relaxation T_2 (spin-spin relaxation) was measured using a CPMG NMR sequence with an interecho spacing, TE , of $0.350 \mu\text{s}$. T_1 and T_2 relaxation time distributions were calculated using multi-exponential fitting routines based on singular value decomposition algorithms (Sezginger, 1991-1994). The reader may find more information on signal conversion in Prammer (1994) or Gallegos and Smith (1988).

Results

Fig. 2 shows the T_1 -relaxation time distributions on one set of measurements performed on the Red Wildmoor sandstone material. The sandstone was loaded under increasing stress levels until it failed at an axial load of 5 MPa. The distributions provide very individual information on compaction and failure of each rock sample. The changes in the distributions are not obvious on first sight. A data reduction evaluating the mean $1/T_1$ relaxation rate for each measurement was applied. After determining the mean T_1 and the relaxation rate $1/T_1$, eq. 4 was applied. Finally, the relaxation rate difference $\Delta 1/T_1$ was plotted versus increasing stress levels, see Fig. 3.

It can be seen that the rate difference $\Delta 1/T_1$ is negative throughout the entire loading process. The rate difference is furthermore decreasing up to 4 MPa axial load, while values beyond 4 MPa are increasing again. T_2 measurements were performed before each T_1 measurement. T_2 Relaxation rate differences were calculated in the same way as the T_1 rate differences. Results of this evaluation are shown in Fig. 4.

Discussion

Decreasing T_1 relaxation rate differences reflect a reduction in surface relaxivity and/or surface to volume ratio, see eq. 3. As the Red Wildmoor sandstone is a rather weakly consolidated sandstone it can be expected that grains will be redistributed and an increasing number of pores will be closed with increasing load. Pore closing starts typically with the smallest pores. The closing of micropores would cause that pore spaces that under unloaded conditions contribute with fast relaxation disappear. In a loaded state, the mean relaxation time shifts, thus, to greater values, i.e. slower relaxation rates. It is therefore valid to interpret the measurements presented in Fig. 3 by the closing of micropores and the compression of the sandstone matrix.

When the axial stress exceeds the strength of grain bonds, they will break and the rock may start failing. New fresh mineral surfaces at broken cementations or grain contacts are generated and the surface relaxivity is assumed to increase. This causes faster relaxation rates. In fact, relaxation rates increase after failure, as seen in Fig. 3 at larger axial stresses.

A similar observation as for longitudinal, T_1 , relaxation can be made for transversal, T_2 , relaxation. As explained in eq. 2, T_2 relaxation is affected by a self-diffusion of the protons in the investigated system, in addition to bulk fluid relaxation and surface relaxation. Fig. 4 shows that the T_2 relaxation rate differences react rather sensitive in an initial loading phase. The sample was here loaded with a 0.02 MPa pre-load before the first measurement was taken. This resulted in a strong decrease in the rate difference. After another 16 hours, another NMR-measurement was performed under the same loading conditions and an increase in the rate difference was observed. Compressing the sample with further increasing axial load causes a rather regular decrease in the relaxation rate, similar to the T_1 measurements.

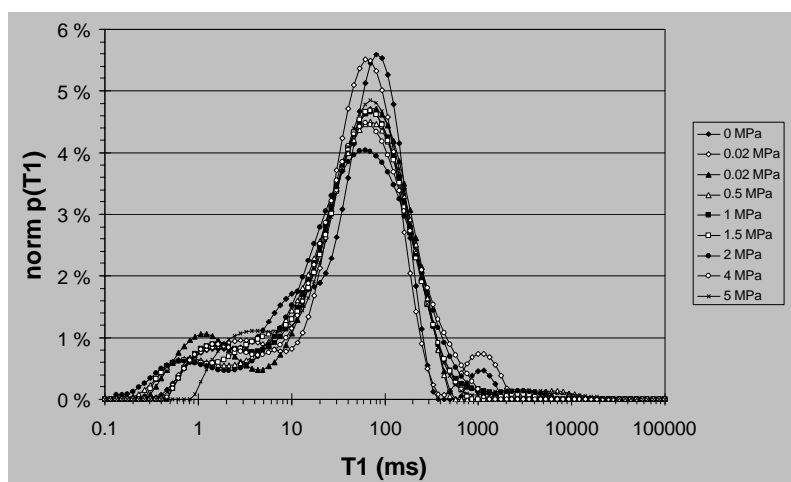


Fig. 2. Relaxation time distributions of ^1H -NMR-measurements (T_1) at 2 MHz proton resonance frequency on Red Wildmoor sandstone sample in different drained, uniaxial compression states.

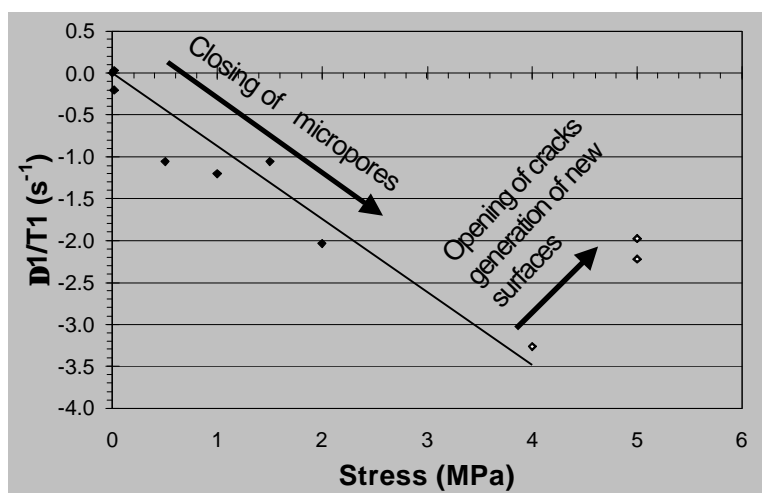


Fig. 3. Difference in the mean relaxation rates, $D1/T_1$, of measurements at increasing axial stress levels compared to the unstressed rock sample. Example Red Wildmoor sandstone.

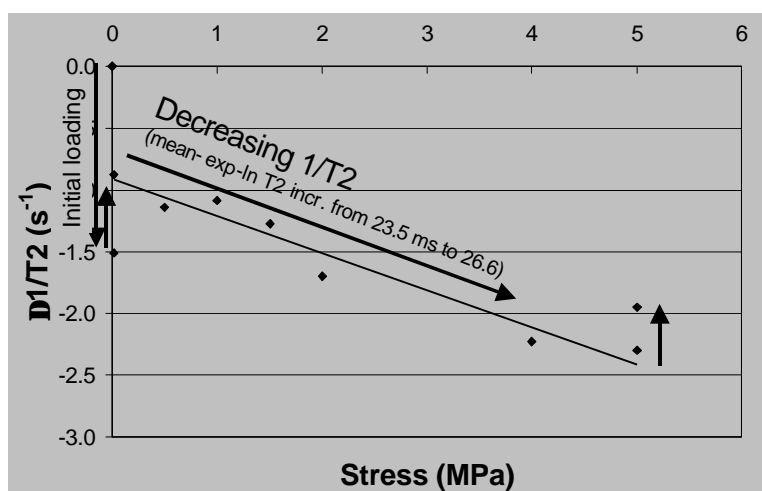


Fig. 4. Difference in the mean relaxation rates, $D1/T_2$, of measurements at increasing axial stress levels compared to the unstressed rock sample. Example Red Wildmoor sandstone.

Measurements on Artificial Sandstone Samples

Method

To simulate the rock mechanical processes and the changes in petrophysical properties of the measurements presented above, a new measurement series was started using artificially consolidated sandstone samples. These samples were prepared with a sample size of 25.4 mm diameter and 40.0 mm lengths using a preparation technique that results in loosely consolidated sandstones with defined crack patterns in terms of number of cracks, thickness of cracks and crack orientation. Samples were made of dry quartz sand with a minimum of contamination and thin aluminium disks to create defined crack patterns. Epoxy glue was used as a cement and an aluminium leaching technique was applied to open the cracks; see Fig. 5. Samples were vacuum saturated in de-ionised water and kept under water throughout storage. During NMR-measurements samples were wrapped in cling-film to avoid evaporation of the pore fluid.

The samples that were used are listed together with relevant information on sample properties in Table 1. The main features that distinguished the samples were;

- crack thickness, 18 μm or 100 μm ,
- crack pattern, plane (perpendicular to the plug axis) or irregular (in $\sim 45^\circ$ or $\sim 315^\circ$ angle to the plug axis),
- number of cracks; sample A1 and A2: no cracks, samples C to F many cracks, sample G and I: one crack; sample H: 5 cracks.

Measurements were performed on a MARAN 10 unit equipped with a superconductive magnet and a 70 mm diameter RF coil. The artificial sandstone samples were carefully centered in the coil with the plug axis parallel to the axis of the RF-coil. Using this set up, it was expected to provide measurements that were not affected by gradients of the external background field B_0 .

The transverse relaxation T_2 was measured using a CPMG NMR sequence with a multi-interecho spacing technique. Measurements were started at a TE of 0.350 μs . Afterwards, measurements were performed at TEs of 700 μs , 1400 μs , 2100 μs and 2800 μs . T_2 relaxation time distributions and mean T_2 values were calculated using the same techniques as mentioned above. Initial measurements to check the quality of the preparation process and the repeatability of the measurements were performed on samples A1 and A2.

Results

The measurements on the two equivalent samples A1 and A2, both with no cracks, are presented in Fig. 6 (Relaxation time distributions at TE=350 μs) and in Table 2 (mean exponential-ln T_2 relaxation rate).

Fig. 6 shows that there are only minor differences in the relaxation time distributions of the two equivalent rock samples. Table 2 indicates that the standard deviation of the measurements at different echo spacing is slightly variable approaching a maximum value of 9.2% in the coefficient of variation (=standard deviation/average). This value is used later to evaluate the quality of the other measurements.

The relaxation time distributions of a series of multi-echo spacing measurements (here sample H) is shown in Fig. 7. The example visualises that the variation of the interecho time TE causes a shift to shorter T_2 . Note that the relaxation rate increases as the relaxation time decreases and that the sensitivity, i.e. the resolution of the peaks in the relaxation time distribution is reduced.

Table 1. Identification and properties of samples used for NMR-measurements on artificial sandstone samples with different crack patterns.

Sample	Diameter (mm)	Length (mm)	Bulk Volume (cm ³)	Porosity (%)	Pore Volume (cm ³)	V of cracks (cm ³)	% crack volume
A1 Dummy	25.07	39.57	19.53	40.5 %	7.90	-	-
C 18 - plane	25.21	40.11	20.02	39.4 %	7.88	4.88E-02	0.62 %
D 100 - plane	25.02	40.16	19.74	38.3 %	7.57	2.71E-01	3.58 %
E 18 - plane	25.15	40.02	19.89	39.4 %	7.84	4.88E-02	0.62 %
F 100 - irreg	25.04	40.06	19.73	40.6 %	8.02	2.71E-01	3.38 %
G 100 - 15 mm	25.00	39.30	19.30	40.7 %	7.85	1.77E-02	0.23 %
H 100 - 5 cracks	25.15	39.90	19.82	40.2 %	7.97	1.15E-02	0.14 %
I 18 - 15 mm	25.00	40.00	19.63	40.3 %	7.91	3.18E-03	0.04 %
A2 Dummy	24.72	40.72	19.54	36.0 %	7.03	-	-
average			19.69		7.77		
stdev			0.217		0.306		
coeff. var			1.1 %		3.9 %		

Table 2. Repeatability of relaxation rate evaluations at different interecho spacing TE.

Mean exp-ln-1/T2	TE=350 μ s	700	1400	2100	2800
A1	2.34E-03	2.77E-03	3.70E-03	4.43E-03	4.83E-03
A2	2.56E-03	3.15E-03	4.04E-03	4.90E-03	5.40E-03
average	2.45E-03	2.96E-03	3.87E-03	4.67E-03	5.12E-03
stdev	1.55E-04	2.73E-04	2.42E-04	3.31E-04	4.02E-04
coeff. of variation	6.3 %	9.2 %	6.2 %	7.1 %	7.9 %

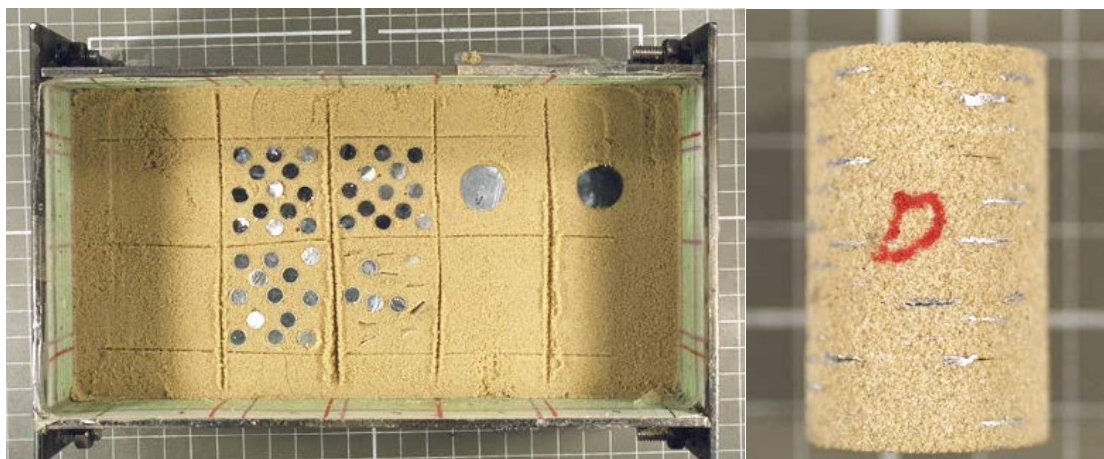


Fig. 5. Preparation of artificial sandstone plugs with cracks.

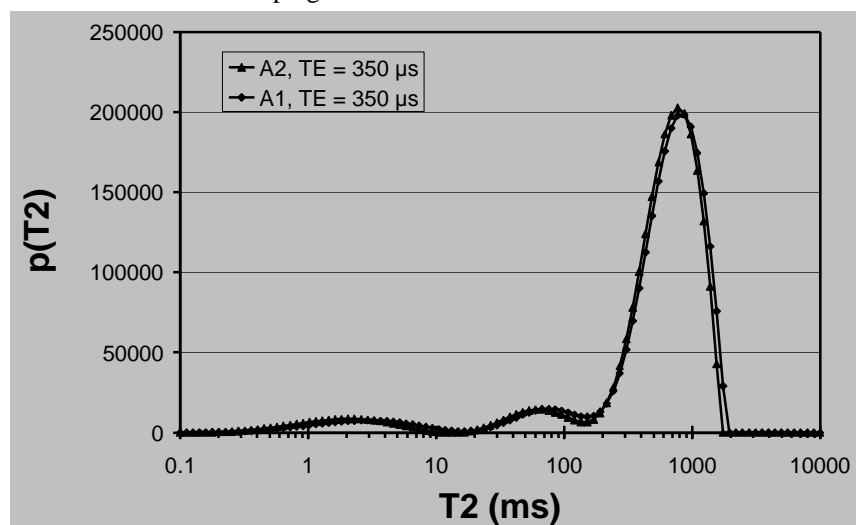


Fig. 6. Relaxation time measurements on two artificial sandstone samples prepared under the same conditions.

Calculating the mean relaxation time T2 from the distributions leads to the observation that T2 follows the same path for all samples, i.e. a longer interecho spacing leads to shorter mean T2. Samples with more cracks and larger cracks are characterised by shorter mean T2, i.e. larger relaxation rates. Fig. 8 shows this effect as an example for samples A1 and F measured at the shortest interecho spacing. The distributions also show that the main peak is broader for the sample with cracks.

Summarising all observations in terms of the mean T2 measurements yields Fig. 9. Using the coefficient of variation found in Table 2 as the potential error to both sides of a measurement, shows that the differences between samples with small (I) or no (A1) crack volume are significant compared to the samples with larger crack volumes.

To estimate the values of the diffusion coefficients for the measurements the following values are used in eq. 5: $\gamma_{1H} = 42.58 \text{ MHz/T} = 4257.60 \text{ Gs}^{-1}$ and $G_n = G_0 = 10 \text{ G/cm} = 1000 \text{ G/m}$. It is assumed that the changes in the internal field gradient G with the interecho spacing are insignificant. The selected value appears reasonable after a review of data published by Appel *et al.* (1999), where internal gradients were measured based on the pulsed field gradient (PFG) NMR-method.

Using the measurements and the assumptions yields values for the diffusion coefficient as presented in Fig. 10. The figure shows that the diffusion coefficient is different for samples with different crack patterns. The coefficient is largest for samples with wide cracks and with a larger numbers of cracks. With increasing TE the diffusion coefficient starts levelling off and approaches a narrow range for all samples. Plotting the diffusion coefficient versus crack volume, as in Fig. 11, demonstrates that the diffusion coefficient is smaller for samples with smaller crack volumes. The values of the diffusion coefficients are in good agreement with the results presented by Appel *et al.* (1999). For comparison, the value for unrestricted self diffusion of water @25°C is $D_0 = 2.3 \times 10^{-5} \text{ cm}^2/\text{s}$. This value should be expected at very short interecho spacings. Apparently, the values calculated for the artificial sandstone samples are in the correct order of magnitude.

Last but not least, in order to understand and demonstrate the compaction and closure of micropores in a sandstone sample as observed in the study of the Red Wildmoor sandstone, an approach was chosen where relaxation rate differences were calculated for all samples using sample F (large and irregular cracks) as a baseline. Plotting the relaxation rate differences versus crack volume, as in Fig. 12, yields a presentation of measurements that appears similar to Fig. 4. Relaxation rate differences decrease with reduced crack volumes. Reduced crack volumes reflect here compaction and crack closure at increasing stress levels.

Discussion

According to Straley *et al.* (1994), T1 and T2 distributions of brine saturated rock samples reflect pore size distributions of the porous matrix. Long relaxation times reflect larger pores, while short relaxation times reflect small pores. A cracks pattern in an otherwise homogeneous porous matrix is intuitively expected to induce slower relaxation, i.e. greater mean relaxation times. Cracks create open spaces in the porous matrix that would correlate to larger pores.

It has been shown that very similar artificial sandstone samples can be generated using the given preparation techniques. The pore fluid in the samples is the same and the samples are prepared of the same material with almost equal pore volumes (coefficient of variation 3.9%, see Table 2). Note that pore volumes do not correlate with the crack volumes. It can therefore safely be assumed that bulk fluid relaxation and surface relaxation are equal for the different samples and that eqs. 4 and 5 are applicable to the described task.

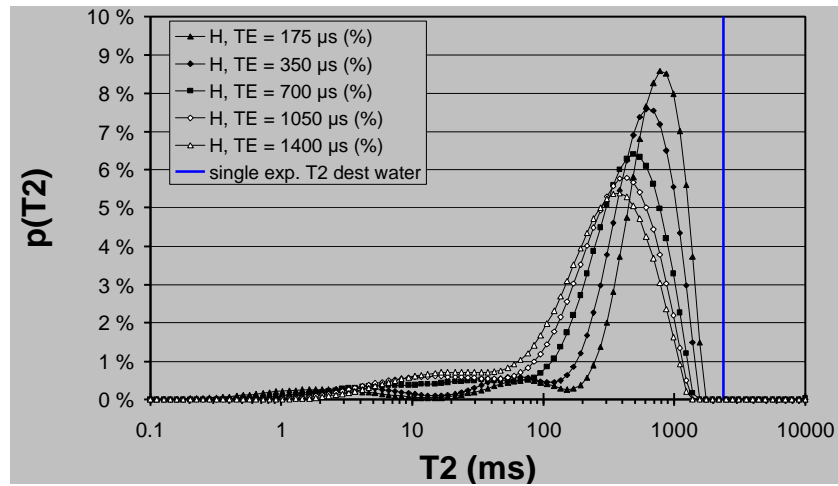


Fig. 7. Relaxation time distributions of multi interecho spacing CPMG measurements (example sample H).

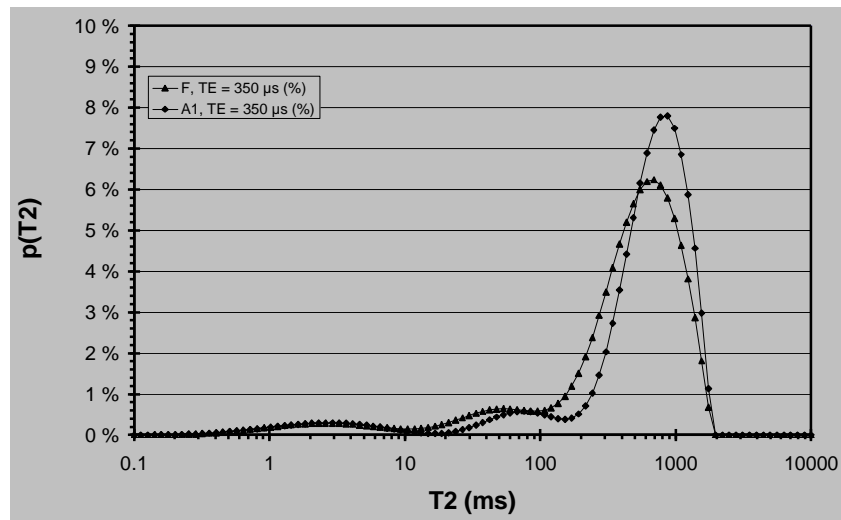


Fig. 8. Relaxation time distributions (T_2) of samples F (many, large cracks) and sample A1 (no cracks) at short interecho spacing $TE=350 \mu s$.

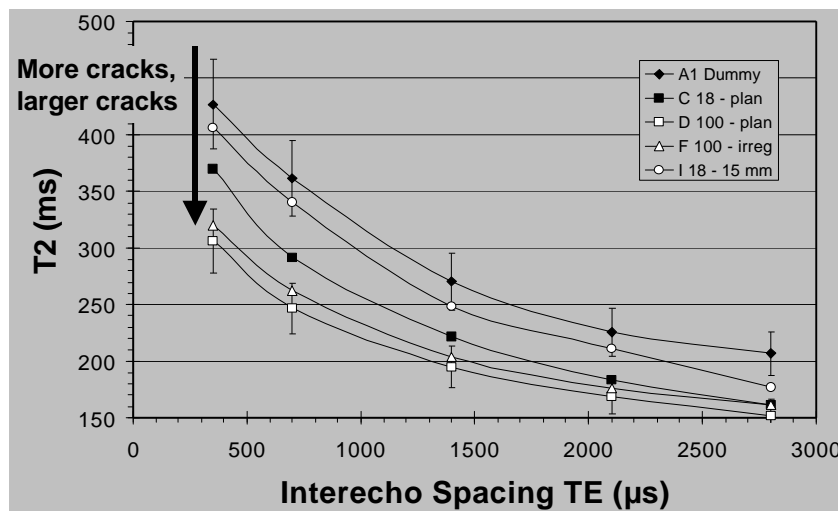


Fig. 9. Summary of the mean exp- $\ln T_2$ values for selected samples at different interecho spacing TE.

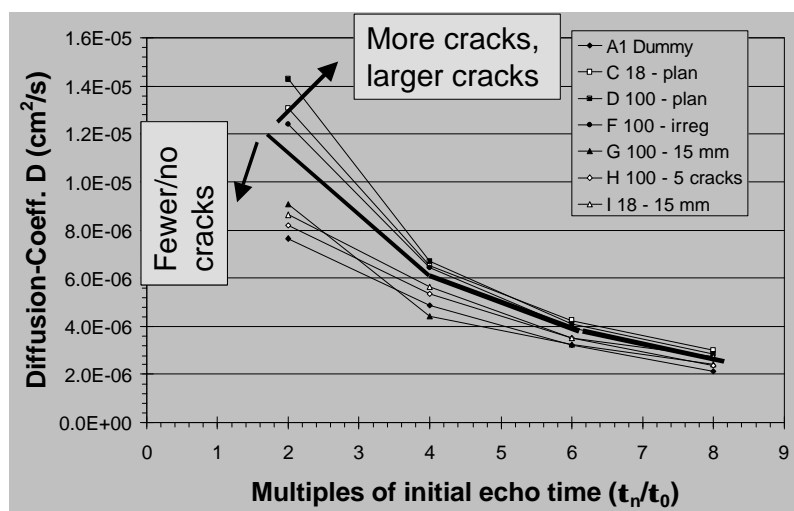


Fig. 10. Estimated diffusion coefficient for artificial sandstone samples prepared with different crack patterns based on multi-echo spacing NMR T2 relaxation time measurements.

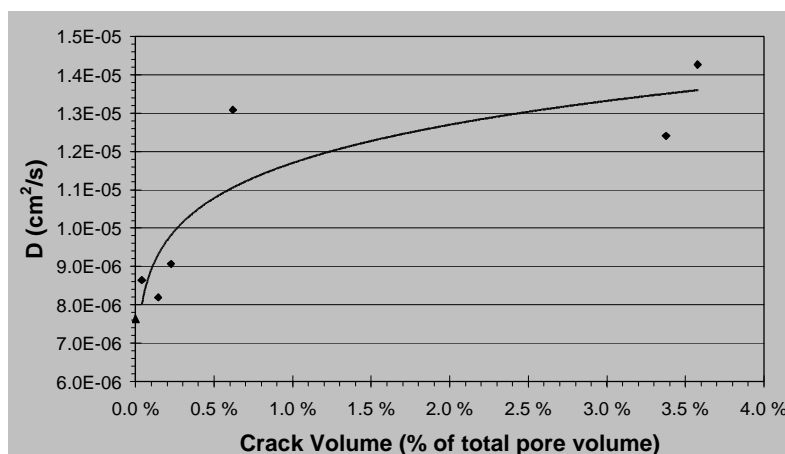


Fig. 11. Plot of the diffusion coefficient D calculated at the interecho spacing of $350 \mu\text{s}$ versus the calculated crack volume of the artificial sandstone samples.

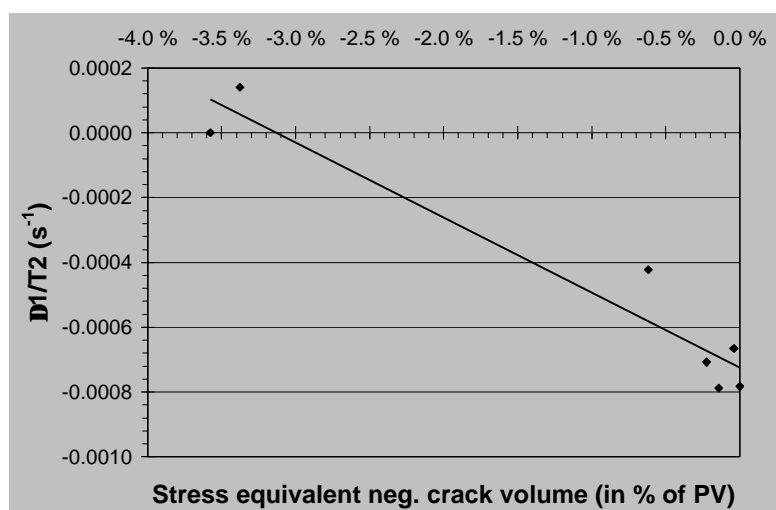


Fig. 12. Relaxation rate difference vs. (negative) crack volume for artificial sandstones with different crack patterns. One sample (ID: F) with the largest crack volume is used as the baseline for calculations. Reduced (negative) crack volumes reflect a process equivalent to compaction through increasing stress.

Also, the assumption that any changes in the internal field gradient G with the interecho spacing are insignificant may hold, as the artificial sandstones were made of clean quartz sand and susceptibility contrasts are small for pure quartz.

Hence, the changes in the relaxation rate $1/T_2$ are entirely related to the crack pattern, the selection of the interecho spacing TE and the diffusion coefficient D. Comparing the dependence of D on TE for different crack patterns shows that increasing crack volumes correlate to significant increases in D.

However, the mean T₂-relaxation time decreases with increasing D, as well as the entire relaxation time spectra broaden but move to shorter relaxation time components. This observation is in contrast to the initial assumption that cracks would induce greater mean relaxation times as they create open spaces in the porous matrix that would correlate to larger pores.

Conclusions

A study on the NMR relaxation response of core plug samples (Red Wildmoor Sandstone) under stress was performed. Attempts were made to explain some of the observations by NMR-measurements on artificial sandstone samples prepared with different, defined crack patterns and crack volumes. The aim of this section is to combine observations made in both parts of the work and discuss the value of the results.

- The compaction of a rock sample may cause closure of micropores. As micropores disappear NMR-relaxation time distributions may shift to greater mean T₁ or T₂ values, as faster relaxing components of the porous matrix associated with micropores disappear.
- When rock samples fail, relaxation rates may increase through the generation of fresh mineral surfaces at broken cementations or grain contacts.
- Development of cracks in a porous matrix affects the contribution of self diffusion in T₂ measurements. The diffusion coefficient, D, can increase with increasing crack volumes.
- Relaxation rates increase with the diffusion coefficient. Hence, cracks can introduce faster relaxation. This observation is in contrary to the initial assumption that cracks would induce slower relaxation as they create open spaces in the porous matrix that would correlate to larger pores.
- The study may serve as a first tool to assess the potential error in the interpretation of NMR downhole measurements performed in formations affected by stress induced cracks or fissures. It may also be helpful to demonstrate and explain dependencies between rock mechanical parameters, routine core analysis measurements and NMR-measurements.

References

- Appel, M., *et al.*, 1999, "Restricted Diffusion and Internal Field Gradients," paper FF presented at the SPWLA 40th Ann. Logging Symp., Oslo, Norway.
- Coates, G.R., *et al.*, 1993, "Restrictive Diffusion from Uniform Gradient NMR Well Logging," paper SPE 26472, ATCE, Oct. 3-6, Houston.
- Gallegos, D.P., and Smith, D.M., 1988, "A NMR-Technique for the Analysis of Pore Structure: Determination of Continuous Pore Size Distributions," *J. Colloid and Interface Sc.*, 122, 1, 03/88.
- Kleinberg, R.L., *et al.*, 1993, "Nuclear Magnetic Resonance of Rocks: T₁ vs. T₂," paper SPE 26470 presented at the 68th ATCE, Oct. 3-6, Houston.
- Prammer, M.G., 1994, "NMR-Pores Size Distributions and Permeability at the Well Site," paper SPE 28368 presented at the 69th ATCE, New Orleans.
- Sezginger, A., 1991-1994, t1heel and t2heel software, Schlumberger-Doll Research.
- Straley, *et al.*, 1994, "Core analysis by low field NMR," paper SCA 9404, proc. SCA Conf., Stavanger.
- van der Zwaag, C., *et al.*, 2000, "NMR Response of Non-Reservoir Fluids in Sandstones and Chalks," Proceedings of the 5th International Meeting on Recent Advances in MR Applications to Porous Media, Bologna, Italy, Oct. 9-11; also published in *Magnetic Resonance Imaging*, Vol. 19, 3/4, 2001.